

Spark Deficient Gabor Frame Provides a Novel Analysis Operator for Compressed Sensing

Vasiliki Kouni

Chair for Mathematics of Information Processing
RWTH Aachen University

Aachen, Germany

kouni@mathc.rwth-aachen.de

Department of Informatics and Telecommunications
National and Kapodistrian University of Athens

Athens, Greece

vicky-kouni@di.uoa.gr

Holger Rauhut

Chair for Mathematics of Information Processing
RWTH Aachen University

Aachen, Germany

rauhut@mathc.rwth-aachen.de

Abstract—The analysis sparsity model is a very effective approach in modern Compressed Sensing applications. Specifically, redundant analysis operators can lead to fewer measurements needed for reconstruction when employing the analysis l_1 -minimization in Compressed Sensing. In this paper, we pick an eigenvector of the Zauner unitary matrix and –under certain assumptions on the ambient dimension– we build a spark deficient Gabor frame. The analysis operator associated with such a spark deficient Gabor frame, is a new (highly) redundant Gabor transform, which we use as a sparsifying transform in Compressed Sensing. We conduct computational experiments –on both synthetic and real-world data– solving the analysis l_1 -minimization problem of Compressed Sensing, with four different choices of analysis operators, including our Gabor analysis operator. The results show that our proposed redundant Gabor transform outperforms –in all cases– Gabor transforms generated by state-of-the-art window vectors of time-frequency analysis.

Index Terms—Compressed Sensing, analysis sparsity, Gabor transform, window vector, spark deficient Gabor frame

I. INTRODUCTION

Context. Compressed Sensing (CS) [1] is a modern technique to recover vectors $x \in \mathbb{C}^L$ from few linear and possibly corrupted measurements $y = Ax + e \in \mathbb{C}^K$, $K < L$. The applications of CS vary from Radar Imaging [2], Cryptography [3] and Telecommunications [4], to Magnetic Resonance Imaging (MRI) [5], Deep Learning [6] and Computer Graphics [7].

Related works. CS heavily relies on sparsity/compressibility of the signal of interest x . A signal x is called *s-sparse* if it has at most s nonzero entries, while it is called *compressible* if it is well approximated by an s -sparse vector. Sparsity models are split in two categories: synthesis sparsity and analysis sparsity. Synthesis sparsity model [8] is by now very well studied [9], [10], [11], [12]. On the other hand, significant research has also been conducted over the last years towards its analysis counterpart [13], [14], [15], [16] (also known as co-sparse model [17]), due

to the flexibility it provides in modelling sparse signals, since it leverages the redundancy of the involved analysis operators. Related work has also demonstrated that if one uses a redundant transform instead of an orthogonal¹ one in analysis CS, the dimension of the optimization problem is smaller [18] and the optimization algorithm used may need less measurements for perfect reconstruction [14].

Motivation. In this work, we are motivated by results of [13], [17], [19] and [14]. These publications propose either analysis operators associated to redundant frames (i.e. matrices whose atoms/rows form a frame of the ambient space) with atoms in general position, or a finite difference operator (associated to the popular method of total variation [20]), in which many linear dependencies appear for large dimensions. In a similar spirit, in this paper we also deploy frames, but we differentiate our approach from the previous works by using *spark deficient* frames. The elements of spark deficient frames are not in general linear position, so we leverage these stronger linear dependencies. To that end, we introduce a novel redundant analysis operator associated with a spark deficient Gabor frame (SDGF). Such a frame can be generated by time-frequency shifts of any eigenvector of the Zauner unitary matrix [21], under certain assumptions. To the best of our knowledge, we are the first to combine analysis CS with spark deficient Gabor analysis operators. Moreover, since Gabor transforms are little explored in terms of CS [22], [12], [23], we compare our proposed Gabor analysis operator to three others, which emerge from state-of-the-art window vectors in time-frequency analysis. Finally, we illustrate the practical importance of our method not only for synthetic data, but also for real-world signals.

Key contributions. Our novelty is twofold: (a) we generate a SDGF based on a window vector, associate this SDGF to a Gabor analysis operator and use the latter as a sparsifying transform in analysis CS (b) we compare numerically our

V. Kouni acknowledges financial support from the German Academic Exchange Service (DAAD)

¹synthesis and analysis models coincide when the analysis operator is orthogonal/unitary

proposed method with three other Gabor analysis operators, based on famous windows of time-frequency analysis, on both synthetic and real-world data. Our experiments show that our method outperforms all others consistently for synthetic and real-world signals.

The rest of the paper is organized as follows: in Section II we give notation, briefly introduce the setup of CS and explain how we tailor it to our purpose. Section III describes Gabor frames and extends to spark deficient ones, building the desirable SDGF and its analysis operator. Section IV contains the results of our numerical experiments. Lastly, in Section V we make some concluding remarks and give potential future directions.

II. COMPRESSED SENSING SETUP

A. Notation

- For a set of indices $N = \{0, 1, \dots, N-1\}$, we write $[N]$.
- (Bra-kets) The set of (column) vectors $|0\rangle, |1\rangle, \dots, |L-1\rangle$ is the standard basis of \mathbb{C}^L .
- We write \mathbb{Z}_L for the ring of residues mod L , that is $\mathbb{Z}_L = \{0 \bmod L, 1 \bmod L, \dots, (L-1) \bmod L\}$.
- We write $a \equiv b \pmod{L}$ for the congruence modulo, where $a, b \in \mathbb{Z}$.
- The support of a signal $x \in \mathbb{C}^L$ is denoted by $\text{supp}(x) = \{i \in [L] : x_i \neq 0\}$. For its cardinality we write $|\text{supp}(x)|$ and if $|\text{supp}(x)| \leq s \ll L$, we call x s -sparse.

B. Analysis Compressed Sensing Formulation

As already described in Section I, the main idea of CS is to reconstruct a signal $x \in \mathbb{C}^L$ from $y = Ax + e \in \mathbb{C}^K$, $K < L$, where A is the so-called measurement matrix and $e \in \mathbb{C}^K$, with $\|e\|_2 \leq \eta$, corresponds to noise. To do so, we will first assume there exists a redundant sparsifying transform $\Phi \in \mathbb{C}^{P \times L}$ ($P > L$) called the analysis operator, such that Φx is (approximately) sparse.

On the other hand, the choice of A is tailored to the application for which CS is employed. For example, in MRI, A is a partial Fourier matrix. There exist conditions on A which ensure exact or approximate reconstruction of x , such as the *null space property* or the *restricted isometry property* [8]. Random Gaussian matrices, whose entries consist of independent random variables following a standard normal distribution, have been proven to work particularly well [8], since they meet the aforementioned conditions. Hence, a random Gaussian measurement matrix A will be our choice in the rest of this paper.

Now, using analysis sparsity in CS, we wish to recover x from y , that is solve the *analysis l_1 -minimization* problem

$$\min_{x \in \mathbb{C}^L} \|\Phi x\|_1 \quad \text{subject to} \quad \|Ax - y\|_2 \leq \eta, \quad (1)$$

or a smoothed version² of it:

$$\min_{x \in \mathbb{C}^L} \|\Phi x\|_1 + \frac{\mu}{2} \|x - x_0\|_2^2 \quad \text{subject to} \quad \|Ax - y\|_2 \leq \eta, \quad (2)$$

²the interested reader can be referred to [24], which explains in detail the reason for the preference in solving (2) instead of (1)

where x_0 denotes an initial guess on x and $\mu > 0$ is a fixed smoothing parameter.

We will devote the next Section to the construction of a suitable analysis transform Φ .

III. GABOR FRAMES

A. Gabor Systems

A *discrete Gabor system* (g, a, b) [25] is defined as a collection of time-frequency shifts of the so-called window vector $g \in \mathbb{C}^L$, expressed as

$$g_{n,m}(l) = e^{2\pi i m b l / L} g(l - na), \quad l \in [L], \quad (3)$$

where a, b denote time and frequency parameters respectively, $n \in [N]$ chosen such that $N = L/a \in \mathbb{N}$ and $m \in [M]$ chosen such that $M = L/b \in \mathbb{N}$ denote time and frequency shift indices respectively. If (3) spans \mathbb{C}^L , it is called *Gabor frame* and an equivalent definition of a frame [26] is given below.

Definition 3.1: Let $L \in \mathbb{N}$ and $(\phi_p)_{p \in P}$ a finite subset of \mathbb{C}^L . If the inequalities

$$c_1 \|x\|_2^2 \leq \sum_{p \in P} |\langle x, \phi_p \rangle|^2 \leq c_2 \|x\|_2^2 \quad (4)$$

hold true for all $x \in \mathbb{C}^L$, for some $0 < c_1 \leq c_2$ (frame bounds), then $(\phi_p)_{p \in P}$ is called a *frame* for \mathbb{C}^L .

The number of elements in (g, a, b) according to (3) is $P = MN = L^2/ab$ and if (g, a, b) is a frame, we have $ab < L$ (we shall refer to this situation from now on as oversampling [27]). A crucial ingredient in order to have good time-frequency resolution of a signal with respect to a Gabor frame, is the appropriate choice of the time-frequency parameters a and b . Apparently, this challenge can only be treated by numerically experimenting with different choices of a, b with respect to L .

B. The Analysis and Synthesis Operator associated with a Gabor frame

We can associate two operators to the Gabor frame (g, a, b) . Let $\Phi_g : \mathbb{C}^L \mapsto \mathbb{C}^{M \times N}$ denote the *Gabor analysis operator* – also known as *digital Gabor transform*³ (DGT) – whose action on a signal $x \in \mathbb{C}^L$ is defined as

$$c_{m,n} = \sum_{l=0}^{L-1} x_l \overline{g(l - na)} e^{-2\pi i m b l / L}, \quad (5)$$

for $m \in [M]$, $n \in [N]$. Then, its adjoint is the *Gabor synthesis operator* $\Phi_g^T : \mathbb{C}^{M \times N} \mapsto \mathbb{C}^L$ whose action on the coefficients $c_{m,n}$ gives

$$x_l = \sum_{n=0}^{N-1} \sum_{m=0}^{M-1} c_{m,n} g(l - na) e^{2\pi i m b l / L}, \quad (6)$$

for $l \in [L]$. Since we will deal with analysis CS in this paper, we will only focus on Φ_g from now on.

³so we will interchangeably use both terms from now on

C. Spark Deficient Gabor Frames

Let us first introduce some basic notions needed in this subsection.

Definition 3.2: The symplectic group $\text{SL}(2, \mathbb{Z}_L)$ consists of all matrices

$$G = \begin{pmatrix} \alpha & \beta \\ \gamma & \delta \end{pmatrix} \quad (7)$$

such that $\alpha, \beta, \gamma, \delta \in \mathbb{Z}_L$ and $\alpha\gamma - \beta\delta \equiv 1 \pmod{L}$. To each such matrix corresponds a unitary given by the explicit formula [28]

$$U_G = \frac{e^{i\theta}}{\sqrt{L}} \sum_{u,v=0}^{L-1} \tau^{\beta^{-1}(\alpha v^2 - 2uv + \delta u^2)} |u\rangle \langle v|, \quad (8)$$

where θ is an arbitrary phase, β^{-1} is the inverse⁴ of $\beta \pmod{L}$ and $\tau = -e^{\frac{i\pi}{L}}$.

Definition 3.3: The *spark* of a set F —denoted by $\text{sp}(F)$ —of P vectors in \mathbb{C}^L is the size of the smallest linearly dependent subset of F . A frame F is full spark if and only if every set of L elements of F is a basis, or equivalently $\text{sp}(F) = L + 1$, otherwise it is spark deficient.

Based on the previous definition, a Gabor frame with $P = L^2/ab$ elements of the form (3) is full spark, if and only if every set of L of its elements is a basis. Now, as proven in [26], almost all window vectors generate full spark Gabor frames, so the SDGFs are generated by exceptional window vectors. Indeed, the following theorem was proven in [28] and informally stated in [29], for the *Zauner* matrix $\mathcal{Z} \in \text{SL}(2, \mathbb{Z}_L)$ given by

$$\mathcal{Z} = \begin{pmatrix} 0 & -1 \\ 1 & -1 \end{pmatrix} \equiv \begin{pmatrix} 0 & L-1 \\ 1 & L-1 \end{pmatrix}. \quad (9)$$

Theorem 3.4 ([28]): Let $L \in \mathbb{Z}$ such that $2 \nmid L$, $3 \mid L$ and L is square-free. Then, all eigenvectors of the Zauner unitary matrix $U_{\mathcal{Z}}$ (produced by combining (8) and (9)), generate spark deficient Gabor frames for \mathbb{C}^L .

Therefore, in order to produce a SDGF and apply its associated analysis operator in CS, we must first choose an ambient dimension L that fits the assumptions of Theorem 3.4. Then, we calculate $U_{\mathcal{Z}}$ using (8) and (9) and in the end, perform its spectral decomposition in order to acquire its eigenvectors. Since all the eigenvectors of $U_{\mathcal{Z}}$ generate SDGFs, we may choose without loss of generality an arbitrary one, which we call *star window* and denote it as g_* from now on. We call the analysis operator associated with such a SDGF *star DGT* and denote it Φ_{g_*} , in order to show the dependance on g_* . We coin the term “star”, due to the slight resemblance of this DGT to a star when plotted in Matlab.

IV. NUMERICAL EXPERIMENTS

A. Signals’ description

We now run experiments on both synthetic and real-world data. The synthetic complex signal *LoSine* [30] is a plain

sine wave. The real-world *Glockenspiel* [31] is a real-world, real-valued audio signal, sampled at 22.05kHz and consists of 231072 samples. For each of the two signals we follow almost the same procedure with minor adaptations, presented in the next subsection.

B. Proposed framework

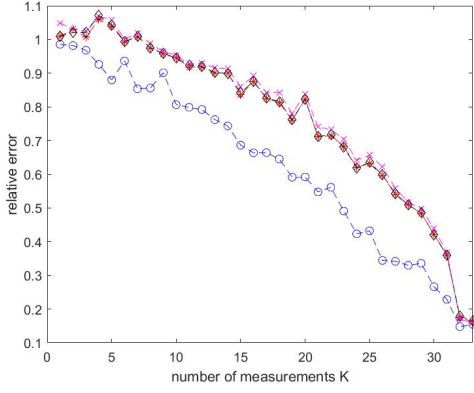
The steps of our method are now summarized below.

- 1) We fix each signal’s dimension L (especially for *Glockenspiel*, we cut it off to its first L th entries) to match the conditions of Theorem 3.4 and set accordingly the time-frequency parameters (a, b) to provide good time-frequency representation of our signals. For each of our signals, we try two different values of L with corresponding a, b , presented in the table of next subsection.
- 2) We initialize each signal and vary the number of measurements K in the range $\{1, 2, \dots, L\}$.
- 3) We use the power iteration method [32] which yields the largest in magnitude eigenvalue and corresponding eigenvector of $U_{\mathcal{Z}}$, then set this eigenvector as our desired window vector g_* .
- 4) For each of the two signals, we construct—using the Matlab package *LTFAT* [33]—four different Gabor frames with their associated analysis operators/DGTs, which go as follows: Φ_{g_1} , Φ_{g_2} , Φ_{g_3} and Φ_{g_*} , corresponding to a Gaussian, a Hann, an iterated sine (for *LoSine*) or a Hamming [25] (for *Glockenspiel*) and the star window vector respectively. In the case of the real-valued *Glockenspiel*: (a) we keep the real part⁵ of g_* (b) we alter the four analysis operators to compute only the DGT coefficients of positive frequencies instead of the full DGT coefficients.
- 5) For each measurement $K \in \{1, 2, \dots, L\}$, we repeat the following procedure 20 times:
 - we draw a standard i.i.d. Gaussian random matrix $A \in \mathbb{C}^{K \times L}$ for *LoSine* and a standard i.i.d. Gaussian random matrix $A \in \mathbb{R}^{K \times L}$ for *Glockenspiel*, then determine the measurement vector $y = Ax$ and add white noise to y ,
 - we solve—using the Matlab packages⁶ *CVX* [34] and *TFOCS* [24] for *LoSine* and *Glockenspiel* respectively—four different instances of (2), one for each of the four DGTs. For *CVX*, we use the *SDPT3* solver, set precision to *best* and initial guess $x_0 = 0$. For each of the instances $i = 1, 2, 3, *$, we set the smoothing parameter $\mu_i = 10^{-5} \|\Phi_i x\|_\infty$, since we noticed an improved performance of the algorithm when μ is a function of Φ_i (the scaling factor 10^{-5} and $\|\cdot\|_\infty$ are simply chosen empirically). For *TFOCS*, we use the *solver_BPDN_W* solver combined with continuation, set $x_0 = 0$, $z_0 = []$, *opts*=[] and for each of the instances

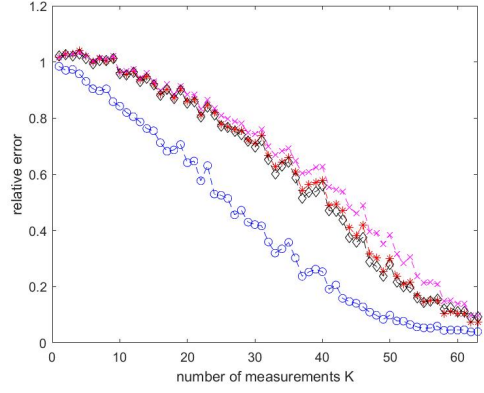
⁵another experiment however, in which we combined a complex g_* with real-valued DGT, resulted in almost the same figure as Fig. 2

⁶we turn to *TFOCS* instead of *CVX*, due to the slow convergence that *CVX* exhibits as the ambient dimension grows larger

⁴ $b\beta^{-1} \equiv 1 \pmod{L}$

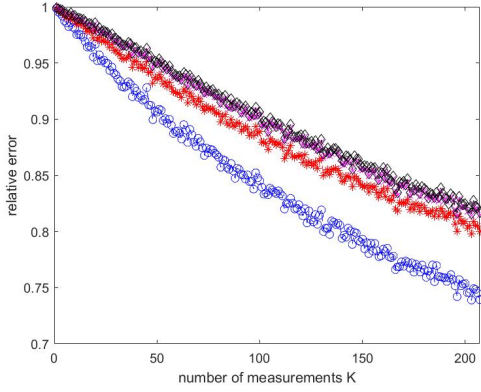


(a) $(L, a, b) = (33, 1, 11)$

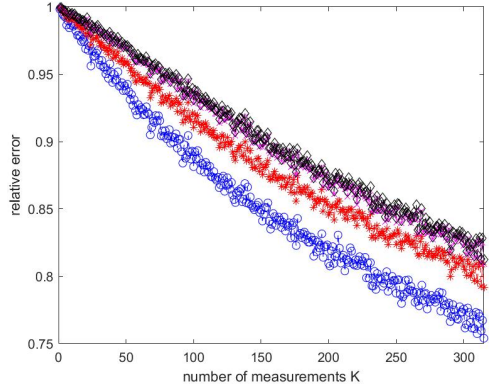


(b) $(L, a, b) = (63, 3, 7)$

Fig. 1: Rate of approximate success for LoSine for different parameters (L, a, b) . Red: Gaussian, magenta: Hann, black: iterated sine, blue: proposed.



(a) $(L, a, b) = (207, 1, 9)$



(b) $(L, a, b) = (315, 1, 7)$

Fig. 2: Rate of approximate success for Glocksenspiel for different parameters (L, a, b) . Red: Gaussian, magenta: Hann, black: Hamming, blue: proposed.

$i = 1, 2, 3, *$, we set –like before– the smoothing parameter $\mu_i = 10^{-5} \|\Phi_i x\|_\infty$,

- from the aforementioned solving procedure, we obtain four different estimators for each x , namely $\hat{x}_1, \hat{x}_2, \hat{x}_3, \hat{x}_*$ and their corresponding relative errors $\|x - \hat{x}_i\|_2 / \|x\|_2, i = 1, 2, 3, *$.

We would like to mention at this point that, since we are interested in a comparison among star Gabor analysis operator generated by g_* and three other Gabor analysis operators –generated by state-of-the-art window vectors– we do not require a specific threshold of perfect reconstruction of x here; we only aim to show how the four previous window vectors affect implicitly the approximate success of (2), as the number of measurements increases.

C. Tables and Figures

Table I summarizes key characteristics of the application of our framework to both signals.

TABLE I: Parameters, window vectors, analysis operators and measurement procedures for synthetic and real-world signals

Parameters	LoSine	Glocksenspiel
(L, a, b)	$(33, 1, 11)$	$(207, 1, 9)$
(L, a, b)	$(63, 3, 7)$	$(315, 1, 7)$
g_1	Gaussian	Gaussian
g_2	Hann	Hann
g_3	iterated sine	Hamming
g_*	star	star (real part)
DGT	complex	real
Package	CVX	TFOCS
A	complex	real
noisy measurements	yes	yes
$\{\mu_i\}_{i=1,2,3,*}$	$10^{-5} \ \Phi_i x\ _\infty$	$10^{-5} \ \Phi_i x\ _\infty$
(x_0, z_0, opts)	$(0, [], [])$	$(0, [], [])$
solver	SDPT3	solver_BPDN_W
continuation	no	yes

The resulting figures on the top of this page, show the relative reconstruction error decay as the number of measurements increases. Fig. 1 demonstrates the success rate of our proposed

DGT (blue line), outperforming the rest of DGTs for the signal LoSine. Similarly, Fig. 2 indicates that our method (again blue line) outperforms the rest of DGTs in the whole range of measurements for the signal Glockenspiel.

V. CONCLUSION AND FUTURE WORK

In the present paper, we took advantage of a window vector to generate a spark deficient Gabor frame and introduced a novel redundant Gabor analysis operator/DGT, namely the star DGT, associated with this SDGF. We then applied the star DGT to analysis Compressed Sensing, along with three other DGTs generated by state-of-the-art window vectors in the field of Gabor Analysis. Our experiments confirm improved performance. The increased amount of linear dependencies provided by this SDGF, yields for both synthetic and real-world data a lower relative reconstruction error of our method compared to the others, as the number of measurements increases. Future directions will be the extension of the present framework to largescale problems (e.g. images or videos). Additionally, it would be interesting to compare this star-DGT to other similar choices of redundant analysis operators (e.g. redundant wavelet transform, shearlets [11] etc.).

REFERENCES

- [1] E. J. Candès, J. Romberg, and T. Tao, "Robust uncertainty principles: Exact signal reconstruction from highly incomplete frequency information," *IEEE Transactions on information theory*, vol. 52, no. 2, pp. 489–509, 2006.
- [2] L. C. Potter, E. Ertin, J. T. Parker, and M. Cetin, "Sparsity and compressed sensing in radar imaging," *Proceedings of the IEEE*, vol. 98, no. 6, pp. 1006–1020, 2010.
- [3] J. Chen, Y. Zhang, L. Qi, C. Fu, and L. Xu, "Exploiting chaos-based compressed sensing and cryptographic algorithm for image encryption and compression," *Optics & Laser Technology*, vol. 99, pp. 238–248, 2018.
- [4] G. C. Alexandropoulos and S. Chouvardas, "Low complexity channel estimation for millimeter wave systems with hybrid A/D antenna processing," in *2016 IEEE Globecom Workshops (GC Wkshps)*. IEEE, 2016, pp. 1–6.
- [5] M. Lustig, D. L. Donoho, J. M. Santos, and J. M. Pauly, "Compressed sensing MRI," *IEEE signal processing magazine*, vol. 25, no. 2, pp. 72–82, 2008.
- [6] Y. Wu, M. Rosca, and T. Lillicrap, "Deep compressed sensing," in *International Conference on Machine Learning*. PMLR, 2019, pp. 6850–6860.
- [7] P. Sen and S. Darabi, "Compressive rendering: A rendering application of compressed sensing," *IEEE Transactions on Visualization and Computer Graphics*, vol. 17, no. 4, pp. 487–499, 2010.
- [8] S. Foucart and H. Rauhut, "A mathematical introduction to compressive sensing," *Bull. Am. Math.*, vol. 54, no. 2017, pp. 151–165, 2017.
- [9] C. Li and B. Adcock, "Compressed sensing with local structure: uniform recovery guarantees for the sparsity in levels class," *Applied and Computational Harmonic Analysis*, vol. 46, no. 3, pp. 453–477, 2019.
- [10] S. Pejoski, V. Kafedziski, and D. Gleich, "Compressed sensing MRI using discrete nonseparable shearlet transform and FISTA," *IEEE Signal Processing Letters*, vol. 22, no. 10, pp. 1566–1570, 2015.
- [11] M. Yuan, B. Yang, Y. Ma, J. Zhang, R. Zhang, and C. Zhang, "Compressed sensing MRI reconstruction from highly undersampled-space data using nonsubsampling shearlet transform sparsity prior," *Mathematical Problems in Engineering*, vol. 2015, 2015.
- [12] P. T. Dao, A. Griffin, and X. J. Li, "Compressed sensing of EEG with Gabor dictionary: Effect of time and frequency resolution," in *2018 40th Annual International Conference of the IEEE Engineering in Medicine and Biology Society (EMBC)*, 2018, pp. 3108–3111.
- [13] M. Kabanava and H. Rauhut, "Cosparsity in compressed sensing," in *Compressed Sensing and Its Applications*. Springer, 2015, pp. 315–339.
- [14] M. Genzel, G. Kutyniok, and M. März, " l_1 -analysis minimization and generalized (co-) sparsity: When does recovery succeed?" *Applied and Computational Harmonic Analysis*, vol. 52, pp. 82–140, 2021.
- [15] M. Kabanava and H. Rauhut, "Analysis l_1 -recovery with frames and Gaussian measurements," *Acta Applicandae Mathematicae*, vol. 140, no. 1, pp. 173–195, 2015.
- [16] E. J. Candès, Y. C. Eldar, D. Needell, and P. Randall, "Compressed sensing with coherent and redundant dictionaries," *Applied and Computational Harmonic Analysis*, vol. 31, no. 1, pp. 59–73, 2011.
- [17] S. Nam, M. E. Davies, M. Elad, and R. Gribonval, "The cosparsity analysis model and algorithms," *Applied and Computational Harmonic Analysis*, vol. 34, no. 1, pp. 30–56, 2013.
- [18] H. Cherkaoui, L. El Gueddari, C. Lazarus, A. Grigis, F. Poupon, A. Vignaud, S. Farrens, J.-L. Starck, and P. Ciuciu, "Analysis vs synthesis-based regularization for combined compressed sensing and parallel MRI reconstruction at 7 tesla," in *2018 26th European Signal Processing Conference (EUSIPCO)*. IEEE, 2018, pp. 36–40.
- [19] F. Krahmer, C. Kruschel, and M. Sandbichler, "Total variation minimization in compressed sensing," in *Compressed Sensing and its Applications*. Springer, 2017, pp. 333–358.
- [20] L. I. Rudin, S. Osher, and E. Fatemi, "Nonlinear total variation based noise removal algorithms," *Physica D: nonlinear phenomena*, vol. 60, no. 1–4, pp. 259–268, 1992.
- [21] G. Zauner, "Quantum designs," Ph.D. dissertation, University of Vienna Vienna, 1999.
- [22] G. E. Pfander and H. Rauhut, "Sparsity in time-frequency representations," *Journal of Fourier Analysis and Applications*, vol. 16, no. 2, pp. 233–260, 2010.
- [23] S. Rajbanshi, G. Tauböck, P. Balazs, and L. D. Abreu, "Random Gabor multipliers for compressive sensing: a simulation study," in *2019 27th European Signal Processing Conference (EUSIPCO)*. IEEE, 2019, pp. 1–5.
- [24] S. R. Becker, E. J. Candès, and M. C. Grant, "Templates for convex cone problems with applications to sparse signal recovery," *Mathematical programming computation*, vol. 3, no. 3, p. 165, 2011.
- [25] P. L. Søndergaard, P. C. Hansen, and O. Christensen, "Finite discrete Gabor analysis," Ph.D. dissertation, Technical University of Denmark, 2007.
- [26] R.-D. Malikiotis, "A note on Gabor frames in finite dimensions," *Applied and Computational Harmonic Analysis*, vol. 38, no. 2, pp. 318–330, 2015.
- [27] S. Paukner, "Foundations of Gabor analysis for image processing," Master's thesis, University of Vienna, 2007.
- [28] H. B. Dang, K. Blanchfield, I. Bengtsson, and D. M. Appleby, "Linear dependencies in Weyl–Heisenberg orbits," *Quantum Information Processing*, vol. 12, no. 11, pp. 3449–3475, 2013.
- [29] R.-D. Malikiotis, "Spark deficient Gabor frames," *Pacific Journal of Mathematics*, vol. 294, no. 1, pp. 159–180, 2018.
- [30] J. B. Buckheit and D. L. Donoho, "Wavelab and reproducible research," in *Wavelets and statistics*. Springer, 1995, pp. 55–81.
- [31] E. G. Birgin, J. M. Martínez, and M. Raydan, "Algorithm 813: SPG—software for convex-constrained optimization," *ACM Transactions on Mathematical Software (TOMS)*, vol. 27, no. 3, pp. 340–349, 2001.
- [32] T. E. Booth, "Power iteration method for the several largest eigenvalues and eigenfunctions," *Nuclear science and engineering*, vol. 154, no. 1, pp. 48–62, 2006.
- [33] Z. Pruša, P. Søndergaard, P. Balazs, and N. Holighaus, "LTFAT: A Matlab/Octave toolbox for sound processing," in *Proc. 10th International Symposium on Computer Music Multidisciplinary Research (CMMR)*, 2013, pp. 299–314.
- [34] M. Grant and S. Boyd, "CVX: Matlab software for disciplined convex programming, version 2.1," 2014.